

Seamless Transition Control in Spring-Legged Quadrotors: A Hybrid Dynamics Perspective with Guaranteed Feasibility

Hongli Li, Botao Zhang, Rui Mao, Tao Wang, and Hui Cheng

Abstract— Legged aerial-terrestrial robots have garnered significant research attention in recent years due to their enhanced environmental adaptability through combined aerial and terrestrial locomotion. However, existing passive spring-legged aerial robots exhibit limited motion versatility, demonstrating single stance gait during ground impacts, which constrains their task adaptability and creates substantial challenges in hybrid trajectory optimization and switching control. To address these difficulties, this work presents a systematic solution to achieve diverse hybrid locomotion. We innovatively establish the differential flatness property for spring-legged quadrotors in both aerial and terrestrial domains, and propose a unified hybrid trajectory optimization framework that generates smooth, agile, and dynamically feasible multi-modal trajectories incorporating diverse stance gait patterns. Furthermore, a hybrid nonlinear model predictive controller with a trajectory extension strategy is developed to enhance hybrid tracking precision and mode transition execution. Compared to existing methods, we achieve a 30% reduction in tracking error during hybrid locomotion while maintaining high-precision foot placement. The source code will be released to benefit the community¹.

I. INTRODUCTION

Aerial-terrestrial robots have achieved ground mobility, such as rolling, jumping, and walking, by integrating various ground robot motion structures, including wheeled and legged mechanisms [1]–[11]. Some studies have focused on aerial robots equipped with legged structures, designed to mimic bird-like flight or jumping modes. These approaches aim to increase movement speed [8], enhance thrust-to-weight ratios [10], and improve energy efficiency [11] during hybrid motions, along with the ability to perform active ground contact tasks such as sampling and manipulation [12].

Despite these advantages, legged aerial robots still face several significant challenges. One major challenge is the under-explored gait diversity for legged aerial-terrestrial robots during stance phases. Some existing methods analyze step-to-step dynamics, and collect terrestrial locomotion data offline to identify periodic orbits [10] [11]. While ensuring stability during jumping or walking cycles, these methods require precise parameter identification, struggle to maintain dynamic feasibility, and lack generalizability to novel gait patterns, which significantly constrains terrestrial mobility capabilities.

Another significant challenge is the lack of a hybrid controller and mode-switching mechanism that are capable of accurately tracking motion trajectories across different

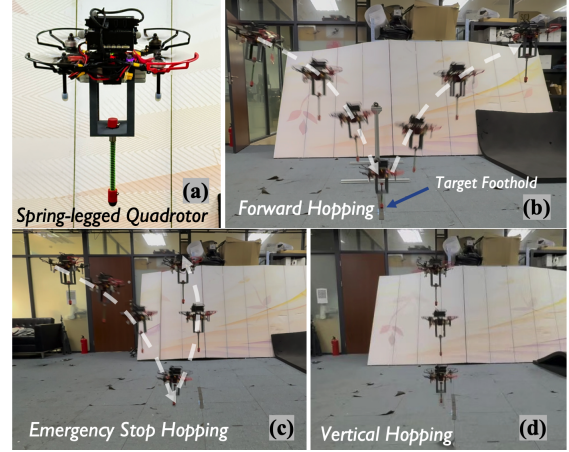


Fig. 1. A quadrotor with a spring leg accurately executes diverse hybrid locomotion, demonstrating seamless mode switching.

modes, as well as adapting to the dynamics specified to each mode. Some legged aerial-terrestrial robots focus only on controlling the velocity or attitude during jumping motions, neglecting the safety and precision in hybrid motions. Additionally, for legged robots, which correspond to a typical state-triggered hybrid dynamic system, the mismatch of the mode switches can cause the system instability or degraded performance.

To address these challenges, this work presents a systematic solution for legged quadrotors hybrid locomotion. First, we derive the differential flatness properties of the spring-legged quadrotors for both the flight and stance phases, demonstrating the controllability throughout all the stages of motion. Second, to ensure the diversity and feasibility of hybrid locomotion, we design a hybrid trajectory optimization method, enforcing dynamics and geometric constraints during flight and stance phases, which thus can generate dynamically feasible trajectories and various stance gaits. Finally, we develop a hybrid nonlinear model predictive controller (HNMPG) with the hybrid trajectory extension strategy. This enables the robot to precisely track the reference trajectory and accurately execute mode transitions. demonstrate our framework's capability to generate multiple types of feasible hybrid trajectories while maintaining precise tracking control.

In summary, our work has three contributions:

- Deriving hybrid differential flatness properties on the spring-legged quadrotor system and developing a flatness-based optimization method, which can generate hybrid trajectories ensuring diversity and dynamic

All authors are with the School of Computer Science and Engineering, Sun Yat-sen University.

Corresponding to chengh9@mail.sysu.edu.cn

¹<https://github.com/sysu19351064/Spring-legged-quadrotor>

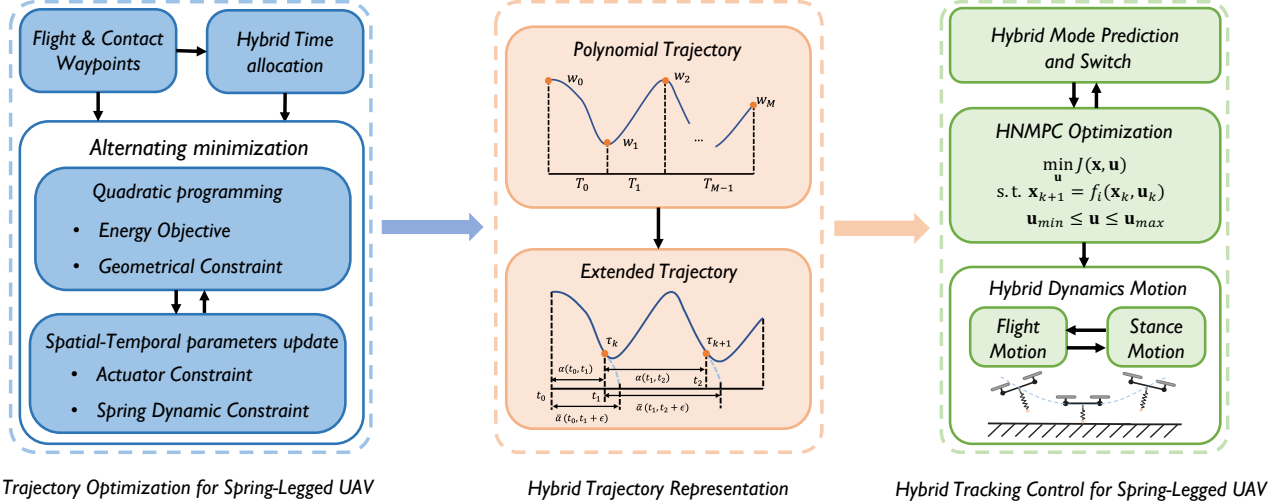


Fig. 2. The system overview. The trajectory optimization module generates smooth, agile, and dynamically feasible multi-modal trajectories incorporating diverse stance gait patterns. The optimal control module tracks hybrid target trajectories and executes mode transitions.

feasibility.

- Designing a HNMPC with a trajectory extension strategy, which can accurately track the reference trajectory and execute mode transitions.
- Extensive simulation and real-world experiments for validating our methods.

The overview of our framework and the symbols used in this paper are shown in Fig. 2 and Table I, respectively.

II. RELATED WORK

Legged aerial-terrestrial robots can be classified into two main categories based on the functionality of their leg structures, i.e., the robots with active legs, and those with passive legs. Active leg structures make it easier for robots to be controlled during walking or jumping [6], [8], [13].

Although active legged robots provide higher mobility and adaptability in complex environments, they complicate the transition between aerial and terrestrial motions, and increase the extra burden on the robot during flight. To address this, some researchers have turned to passive leg structures, using elastic materials to eliminate additional actuators and simplify the design. Zhu et al. [9] incorporated a passive spring leg structure in a quadrotor, reducing energy loss during ground contact. Wang et al. [10] used spring compression to enhance the quadrotor's load capacity during jumps. Mark et al. [12] proposed a novel collision response strategy, converting collision impulses into restorative moments through spring leg compression, enabling rapid post-impact flight stabilization.

For passive-legged aerial-terrestrial robots during jumping motions, researchers often treat the system as either uncontrollable or underactuated, analyzing the post-collision state through the ground reaction impulse estimation [10] [11] while focusing primarily on the stability of the bouncing motion. Additionally, Bai et al. [11] conducted systematic jumping experiments (over 130 trials) to identify stable trajectories for legged quadrotors. Zeng et al. [14] applied

TABLE I. SYMBOLS USED IN THIS PAPER

$\mathbf{e}_x^W, \mathbf{e}_y^W, \mathbf{e}_z^W \in \mathbb{R}^3$	Unit vector in the world frame
$\mathbf{r} \in \mathbb{R}^3$	Position of quadrotor in Cartesian coordinates
$x, y, z \in \mathbb{R}$	Position of the spring leg
$x_t, y_t, z_t \in \mathbb{R}$	Position of the spring leg toe
$x_s, y_s, z_s \in \mathbb{R}$	Position of quadrotor in stance frame
$\mathbf{R} \in \mathcal{SO}(3)$	Orientation of the quadrotor
$(l, \varphi, \theta) \in \mathbb{R}^+ \times \mathcal{S}^2$	Position of quadrotor in spherical coordinates
$\boldsymbol{\omega} \in \mathbb{R}^3$	Angular velocity of quadrotor
$m \in \mathbb{R}$	Mass of quadrotor
$\mathbf{M} \in \mathbb{R}^{3 \times 3}$	Inertia matrix of quadrotor
$f \in \mathbb{R}$	Collective thrust of quadrotor
$\boldsymbol{\tau} \in \mathbb{R}^3$	Torque vector of quadrotor
$l_0 \in \mathbb{R}$	Natural length of the spring leg
$k \in \mathbb{R}$	Spring stiffness of the spring leg

data-driven methods to model the underlying variations in stance dynamics.

While current approaches exhibit notable motion performance and application prospects for spring-legged quadrotors, they neglect to incorporate rotor dynamics during the stance phase and struggling to generate environmentally adaptive, dynamically feasible gaits. This limitation not only confines operations to obstacle-sparse domains but also fundamentally prevents the execution of precision-critical terrestrial operations such as targeted soil sampling or agricultural seeding. Therefore, different from these methods, we propose a novel optimization and controller framework, that can take into account the collective actuation control of rotors and spring leg.

III. HYBRID MODEL DEVELOPMENT

A. The Flight Dynamics

When the spring-legged quadrotor is flying, its leg springs generally remain at their natural length. Consequently, the leg assemblies and the quadrotor body can be treated as one rigid unit. The equations of motion for the robot in the flight mode are obtained as:

$$\ddot{\mathbf{r}} = -mg\mathbf{e}_z^W + f\mathbf{R}\mathbf{e}_z^W, \quad (1a)$$

$$\mathbf{M}\dot{\boldsymbol{\omega}} = \boldsymbol{\tau} - \boldsymbol{\omega} \times \mathbf{M}\boldsymbol{\omega}. \quad (1b)$$

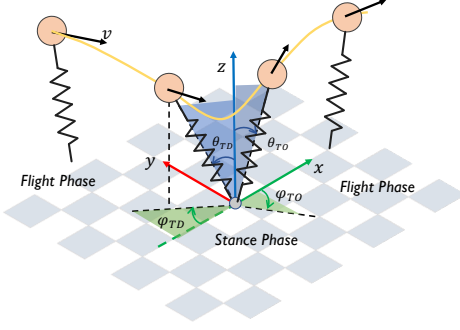


Fig. 3. Hybrid motion of spring-legged quadrotors. During the stance phase, the spring-legged mechanism's foot contact point typically maintains non-slip ground interaction through static friction.

During the flight phase, the state of spring-legged quadrotor is $\mathbf{x}_f = [\mathbf{r}, \mathbf{R}, \dot{\mathbf{r}}, \boldsymbol{\omega}]$. The stance dynamics are triggered when the ground contact occurs at the spring leg toes. This dynamics transition mechanism can be formally defined by the triggering event:

$$\mathcal{S}_{\text{flight} \leftrightarrow \text{stance}} = \{\mathbf{r}^T \mathbf{e}_z^W - l_0 \mathbf{R}_{3,3} \leq 0\}. \quad (2)$$

B. The Stance Dynamics

As shown in Fig. 3, during the stance mode, the non-sliding contact at the foot of the spring leg with the ground introduces holonomic constraints [10], reducing the degrees of freedom. This prompts us to reparameterize the state of spring-legged quadrotors into $\mathbf{x}_s = [l, \varphi, \theta, \dot{l}, \dot{\varphi}, \dot{\theta}]$ within the stance spherical coordinates oriented from the foot of spring leg. To analyze the continuous dynamics, we introduce a rotors spring loaded inverted pendulum (SLIP) model [15], considering the collective effects of the four rotors, thereby establishing a complete dynamic model, as shown in the following equations.

$$m(\ddot{l} - l\dot{\theta}^2 - l\dot{\varphi}^2 \sin^2 \theta) = k(l_0 - l) + f - mg \cos \theta, \quad (3a)$$

$$m(l^2\ddot{\theta} + 2l\dot{l}\dot{\theta} - l^2\dot{\varphi}^2 \sin \theta \cos \theta) = \tau_\theta + mgl \sin \theta, \quad (3b)$$

$$m(l^2\ddot{\varphi} \sin^2 \theta + 2l^2\dot{\varphi}\dot{\theta} \sin \theta \cos \theta + 2l\dot{l}\dot{\varphi} \sin^2 \theta) = \tau_\varphi, \quad (3c)$$

$$M_{zz}\ddot{\psi} = \tau_\psi. \quad (3d)$$

During the stance phase, we decouple rotational dynamics about the body's z-axis from other system states through kinematic constraints, prioritizing planar motion control, as shown in Eq. (3d). The torque control inputs τ_φ and τ_θ represent rotational components about the x-axis and y-axis respectively in the stance frame which can be transformed from the body frame. The flight-to-stance transition triggering function described in Eq. (2) has its reciprocal formulation for stance-to-flight switching, governed by the condition:

$$\mathcal{S}_{\text{stance} \leftrightarrow \text{flight}} = \{l - l_0 \geq 0, \dot{l} > 0\}. \quad (4)$$

The proposed framework for characterizing the hybrid dynamics of spring-legged quadrotors enables smooth mode transitions through two continuous dynamic modes with compatible triggering functions. This formulation ensures

state continuity during dynamic switching, effectively eliminating the unphysical state jumps observed in spring-legged quadrotor systems.

C. The Comprehensive Differential Flatness

By leveraging differential relationships between the stance orthogonal and polar coordinate systems, the state of stance dynamics can be formulated as:

$$\mathbf{I}_{sf} : \begin{cases} l = \sqrt{x_s^2 + y_s^2 + z_s^2}, \\ \varphi = \arctan\left(\frac{y_s}{x_s}\right), \\ \theta = \arctan\left(\frac{\sqrt{x_s^2 + y_s^2}}{z_s}\right), \\ \dot{l} = \frac{x_s \dot{x}_s + y_s \dot{y}_s + z_s \dot{z}_s}{\sqrt{x_s^2 + y_s^2 + z_s^2}}, \\ \dot{\varphi} = \frac{x_s \dot{y}_s - y_s \dot{x}_s}{x_s^2 + y_s^2}, \\ \dot{\theta} = \frac{(x_s \dot{x}_s + y_s \dot{y}_s)z_s}{(x_s^2 + y_s^2 + z_s^2)\sqrt{x_s^2 + y_s^2}} - \frac{\dot{z}_s \sqrt{x_s^2 + y_s^2}}{x_s^2 + y_s^2 + z_s^2}. \end{cases} \quad (5)$$

The coordinate variables $[x_s, y_s, z_s]$ become kinematically equivalent to the world frame coordinates $[x, y, z]$ during the stance phase, as the spring leg foot maintains fixed ground contact.

We will demonstrate, for the first time, the differential flatness properties of the spring-loaded inverted pendulum model driven solely by four rotors during both flight and stance dynamics. This reduces the dimensionality of the nonlinear system, revealing the system's controllability and enabling trajectory optimization.

The differential flatness property of the classic quadrotor dynamics has been elucidated in [16]. By selecting four flat outputs $[x, y, z, \psi]$ and their derivatives, all other state variables of quadrotors can be expressed.

Analogously, the rotors SLIP model of the spring-legged quadrotors during the stance phase can also represent all the state variables using the flat outputs $[x, y, z]$ and their derivatives, as shown in Eq. 5. And also, the control input variables can also be expressed in terms of the flat outputs:

$$\begin{aligned} f &= m \frac{x_s \ddot{x}_s + y_s \ddot{y}_s + z_s \ddot{z}_s + gz_s}{\sqrt{x_s^2 + y_s^2 + z_s^2}} \\ &\quad + k(\sqrt{x_s^2 + y_s^2 + z_s^2} - l_0), \\ \tau_\varphi &= -m \ddot{x}_s y_s + m \ddot{y}_s x_s, \\ \tau_\theta &= m \frac{\ddot{x}_s x_s z_s + \ddot{y}_s y_s z_s - \ddot{z}_s(x_s^2 + y_s^2) - g(x_s^2 + y_s^2)}{\sqrt{x_s^2 + y_s^2}}. \end{aligned} \quad (6)$$

For comprehensive theoretical proofs, refer to the supplementary technical material². In conclusion, the hybrid dynamics of spring-legged quadrotors can be universally represented by a shared set of flat outputs $[x, y, z, \psi]$. The hybrid differential flatness effectively simplifies the trajectory optimization task by reducing the size of the full-state trajectory optimization problem to that of the flat output space while still satisfying the nonlinear dynamic constraints.

²https://github.com/sysu19351064/Spring-legged-quadrotor/blob/main/rotors_SLIP_differential_flatness_provement.pdf

IV. HYBRID TRAJECTORY OPTIMIZATION

A. The Nonlinear Optimization Construction

In each dimension of the flat output variable space, the overall robot trajectory is represented using M polynomial functions of degree N . In flight and stance mode, each trajectory can be expressed as $p(t) = \mathbf{c}^T \beta(t)$, $t \in [0, T]$. Here, $\mathbf{c} \in \mathcal{R}^{(N+1) \times 3}$ is the coefficient matrix, T is the duration, and $\beta(t) = (1, t, t_2, \dots, t_N)^T$ is a basis function.

The constrained optimization problem with energy minimization is written as:

$$\min_{\mathbf{c}, \mathbf{T}} J(\mathbf{c}, \mathbf{T}) = \sum_{i=1}^M \int_0^{t_0} p^{(s)}(t) Q_J p^{(s)}(t) dt, \quad (7a)$$

$$\text{s.t. } p_1^{s-1}(0) = p_0, p_M^{s-1}(t_M) = p_f, \quad (7b)$$

$$p_i^{s-1}(t_i) = p_{i+1}^{s-1}(0), \quad (7c)$$

$$C_b(p_i(t), p_i^{(1)}(t), \dots, p_i^{(s)}(t)) \leq 0. \quad (7d)$$

Here, (7b) and (7c) represent the geometrical constraints and continuity constraints of each trajectory segment, respectively. Based on the analysis of the continuous dynamics from (Sect. III-A and III-B), the adjacent flight and stance trajectories fully adhere to these constraints. (7d) represents the set of all dynamic constraints, which differ based on the flight mode and stance mode.

B. The Geometrical Constraint

The position, velocity, and higher-order derivative constraints of waypoints can be formulated as geometrical constraints for the polynomial trajectory optimization. However, for a stance trajectory segment, the geometrical constraints of touchdown (TD) and takeoff (TO) waypoints cannot be explicitly predefined. Leveraging the differential flatness theory of legged quadrotor systems, we derive the corresponding flat output geometrical constraints $[p(t), p^{(1)}(t), \dots, p^{(s)}(t)]$ from the initial constraints of TD and TO waypoints, which are described in $[l(t), \varphi(t), \theta(t), \psi(t)]$ and their higher-order derivative. For instance, the position constraint can be derived from:

$$\begin{cases} x = x_t + l_0 \sin \theta \cos \varphi, \\ y = y_t + l_0 \sin \theta \sin \varphi, \\ z = z_t + l_0 \cos \theta, \end{cases} \quad (8)$$

where $[l_0, \varphi, \theta]$ represents the natural leg length, splay angle, and swept angle of TD and TO waypoints. Our trajectory optimization framework systematically generates diverse gait patterns by configuring various geometrical conditions of TD and TO waypoints.

C. The Hybrid Dynamical Feasibility Constraint

While differential flatness theory eliminates the need to explicitly handle system dynamics equations, it is still crucial to incorporate flight and stance dynamics constraints into the trajectory optimization framework to ensure the physical feasibility of the generated trajectories.

In physical robotic systems, the thrust vector and torque of quadrotor actuators are constrained by their physical

limitations. The flight dynamic equation is formulated in (1). Directly incorporating thrust constraints as hard boundaries into the optimization framework can substantially complicate the computation. Nevertheless, imposing bound constraints on trajectory higher-order derivatives (e.g., the velocity $v_i(t) \in [v_{min}, v_{max}]$ and acceleration $a_i(t) \in [a_{min}, a_{max}]$) can indirectly ensure the dynamic feasibility in the flat output space [16].

During the stance phase, the collective rotor thrust model is formulated as:

$$f = m \underbrace{\frac{x_s \ddot{x}_s + y_s \ddot{y}_s + z_s \ddot{z}_s + g z_s}{l}}_{\text{acceleration term}} + k(l - l_0). \quad (9)$$

This formulation reveals that the thrust is determined not only by the body acceleration, but also by the force stored in the spring. This constraint characterizes both the dynamic limitations of the actuators and the intrinsic properties of the springs. Moreover, the time-varying spring compression introduces a strong nonlinear coupling, rendering a mere acceleration constraint which can be insufficient to ensure the overall dynamic feasibility.

D. An Alternating Trajectory Optimization

To simplify the optimization for the hybrid dynamical system trajectory, this paper introduces a decoupled optimization framework: (i) Phase I generates geometrically feasible trajectories by quadratic programming (QP), (ii) Phase II verifies the hybrid nonlinear dynamic feasibility and updates spatial-temporal parameters based on the violation of constraints.

a) QP with Geometrical Constraints

The modified trajectory optimization problem (7) by neglecting the dynamic constraints (7d) can be formulated as a convex QP problem. A proper time allocation plays a crucial role in enhancing the quality of the optimized trajectory. For the flight phase, existing methods such as the trapezoidal time allocation are typically employed, whereas for the stance phase, the trajectory duration is allocated based on the half-period of the simple harmonic motion of a spring-mass system:

$$\begin{cases} T_{flight} = \frac{\Delta s_i}{0.5(v_{max} + v_{min})}, \\ T_{stance} = \pi \sqrt{\frac{m}{k}}. \end{cases} \quad (10)$$

Then geometrical equality-constrained QP formulation can be reformulated as the unconstrained QP, enabling closed-form solutions through quadratic programming duality principles [17].

b) The Dynamics Check and Parameter Update

Upon solving the boundary-constrained trajectory optimization, spline parameters for both flight and stance phases are determined, followed by hybrid dynamical feasibility verification. For the flight phase, feasibility checking reduces to trajectory derivative extremum checking. And the trajectory timing is then linearly adjusted based on the severity of any constraint violations [16] [18].

In the stance phase, as illustrated in Fig. 4, there is a clear relationship between the trajectory's spatiotemporal

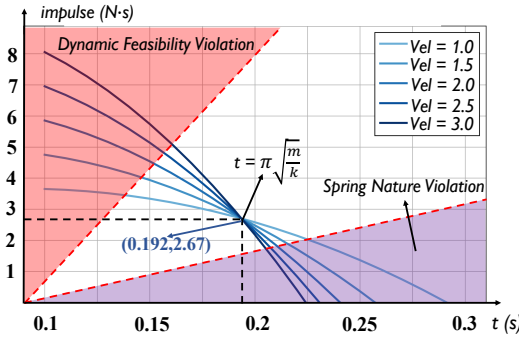


Fig. 4. Illustration of the relationship between the rotors impulse and spatial-temporal parameters during the symmetric stance gait optimization. The model incorporates a robot mass of 1.5 kg and spring stiffness coefficients of 400 N/m. For stance gaits with different initial velocities, the total rotor thrust impulse demonstrates an inverse relationship with gait duration

parameters, rotors impulse, and constraint violation. We compute the cumulative impulse generated by the thrust of quadrotors during the stance gait $I = \int f dt$, as impulse quantification provides a precise evaluation of movement contributions during transient collision phases. Our constraint analysis indicates the updating direction of temporal parameters. In other words, if the duration is too short, the system experiences abrupt accelerations; if it is too long, the intrinsic behavior of the spring mechanism is compromised. Both extreme scenarios contribute to the violation of the stance dynamic feasibility and spring nature. Consequently, we design a heuristic adjustment strategy:

$$T_{stance}^{k+1} = \begin{cases} T_{stance}^k(1 + \eta), & C_b(\cdot) \leq 0 \\ T_{stance}^k(1 + \eta \cdot \text{sgn}(\Delta C^k)), & C_b(\cdot) > 0 \end{cases} \quad (11)$$

where η denotes the adaptive step-size coefficient and ΔC^k represents the stance dynamic constraint violation at the k -th iteration. Subsequently, the updated time allocation is re-incorporated into the previous QP problem, yielding a new set of spline parameters and initiating another iteration of trajectory optimization, until all the constraints are met.

V. HYBRID SYSTEM CONTROLLER DESIGN

A. The HNMPC With Spring State

To enhance the trajectory tracking accuracy and dynamic robustness of spring-legged quadrotors in multimodal locomotion including different stance gait, this work proposes an HNMPC framework that achieves multi-phase trajectory prediction and control through real-time switching between flight and stance dynamic models.

$$\begin{aligned} \min_{\mathbf{u}} J &= \frac{1}{2} \sum_{k=0}^{N-1} (\|\tilde{\mathbf{x}}(k)\|_{\mathbf{Q}_k}^2 + \|\tilde{\mathbf{u}}(k)\|_{\mathbf{R}_k}^2) + \frac{1}{2} \|\tilde{\mathbf{x}}(N)\|_{\mathbf{Q}_N}^2, \\ \text{s.t. } &\mathbf{x}(0) = \mathbf{x}_0, \\ &\mathbf{x}(k+1) = f_i(\mathbf{x}(k), \mathbf{u}(k)), \text{ hybrid dynamics constraint,} \\ &\mathbf{h}(\mathbf{x}(k), \mathbf{u}(k)) \geq 0, \text{ state-input constraint,} \\ &\mathbf{Q}_k \succeq 0, \mathbf{R}_k \succeq 0, \mathbf{Q}_N \succ 0, \end{aligned} \quad (12)$$

where $\tilde{\mathbf{x}}(i) = \mathbf{x}(i) - \mathbf{x}_{ref}(i)$ and $\tilde{\mathbf{u}}(i) = \mathbf{u}(i) - \mathbf{u}_{ref}(i)$, \mathbf{x}_{ref} and \mathbf{u}_{ref} are the desired state and control input trajectory, respectively; System state is \mathbf{x}_f or \mathbf{x}_s based on the current mode; Control input is $\mathbf{u} = [f, \tau]$; N is the prediction horizon; \mathbf{Q}_k and \mathbf{R}_k are the state and control input weighting matrices at k step, respectively.

The framework explicitly incorporates spring compression dynamics into the HNMPC formulation, enabling simultaneous prediction of contact transition sequences, and compensating for spring force disturbances in the rotor thrust through feedforward control, effectively suppressing thrust overshooting when tracking high-acceleration reference trajectories.

B. The Hybrid Trajectory Extension

The trajectory tracking accuracy of spring-legged quadrotors depends not only on the tracking controller performance in individual motion modes but more crucially on the mode transition timing matching degree. Albeit the hybrid motion mode sequences and corresponding dynamically feasible reference trajectories can be obtained through optimization, the asynchrony between actual dynamics switching instants (triggered by leg contact states) and preset switching times in reference trajectories can cause severe model mismatches. When the stance phase in the reference trajectory precedes the actual dynamic switching, the quadrotor is forced to track jumping trajectories but actually in flight dynamics, which can incur velocity step changes and surges in energy loss.

To address this time-varying model mismatch, we propose a hybrid dynamics adaptive trajectory extension method based on the extended trajectory theory from [19]. Given a reference trajectory $\alpha(t)$ with preset switching instant $\tau \in [t_0, t_1]$, we use $\alpha(t_0, \tau)$ to denote the pre-event trajectory and $\alpha(\tau, t_1)$ to represent the post-event trajectory. The pre-event and post-event trajectories are extended based on the current state and dynamics, resulting in $\bar{\alpha}(t_0, \tau + \epsilon)$ and $\bar{\alpha}(\tau - \epsilon, t_1)$. The length ϵ is usually decided by the time horizon of the optimal control problem. By leveraging the analytical extension properties of piecewise polynomial splines, the extended polynomial trajectory satisfies dynamics feasibility constraints without solving again optimization problems.

Accordingly, the extended trajectory is incorporated into the definition of the trajectory tracking error for the optimal control problem. As a result, the new reference trajectory can be expressed as follows:

$$\mathbf{x}(t, t + \epsilon) = \begin{cases} \bar{\mathbf{x}}(t, t + \epsilon), & t < \tau \\ \mathbf{x}(t, t + \epsilon), & t > \tau \end{cases} \quad (13)$$

which means that the controller will continuously track the extended trajectory corresponding to a single mode, ignoring the mode transition in the original reference trajectory until an actual triggering event occurs in the robot.

VI. EXPERIMENTS

A. The System Setup

The experimental platform employs a spring-legged quadrotor (total mass 1.5 kg) with 400 N/m stiffness springs

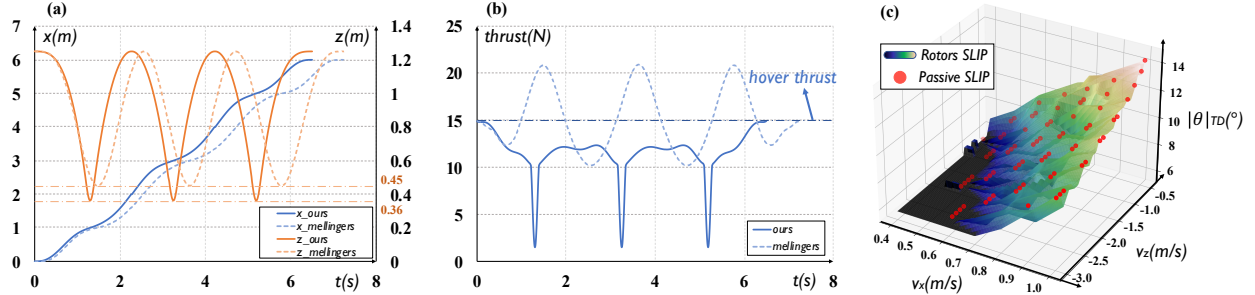


Fig. 5. Comprehensive Comparison of Trajectory Optimization Methods:(a) presents the comparison of position trajectory analyses; (b) demonstrates rotor thrust profile evaluations; (c) illustrates the comparison of symmetric gait solution space distributions during stance phases.

and 0.5/0.4 m light 3D-printed telescopic legs. The hardware for the spring legged quadrotor system is composed of a PX4 flight controller and an onboard computer (DJI Manifold 2 C). We utilize a motion capture system (MoCap) fused with IMU to provide the position of quadrotors and the state of the spring leg. All the simulation experiments are conducted on the computer with an Intel Core i7-13700F CPU under Gazebo simulation environment with the robot model from Rotors [20]. The optimization of the trajectories is implemented through NLOpt [21]. The implementation of HNMPC method is based on the OCS2 toolbox [22].

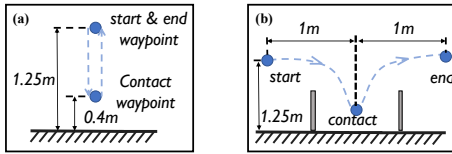


Fig. 6. Experiment Scenario: (a) The z-axis vertical reciprocating hopping; (b) The x-z plane forward hopping with target foothold.

B. The Validation of Optimized Hybrid Trajectory

We compare our optimization method with some SOTA flatness-based methods without considering elastic contact, i.e., Richter [17] 's method and Mellinger [16] 's method. Richter iteratively optimizes the trajectory duration using gradient descent to find the optimal trajectory, while Mellinger rescales the duration based on the extent of constraint violations in the higher-order derivatives.

We design two test scenarios, and their schematic diagrams are provided in Fig. 6. Based on the navigation waypoints in each scenario, the baselines and our method are evaluated through multiple trajectory optimizations under conditions with a body speed limit of [2.0, 2.5]m/s and acceleration constraints from rotor thrust in the range of [3.0, 4.0]m/s².

Three metrics are employed to evaluate the trajectory optimization method: computation time (reflecting optimization efficiency), trajectory duration (indicating motion agility), and rotor impulse (quantifying thrust impact on system dynamics), with all three metrics following the lower-is-better principle.

By comparing the trajectory duration and rotors thrust in both scenarios, we find that our trajectories not only enable more agile maneuvers (17% less time) but also need 37% less rotors impulse. This enhanced performance

TABLE II. A Comparison of Trajectory Optimization Methods

Scenario	Metrics ↓	Mellinger	Richter	Ours
(a)	Computation Time(s)	0.051	0.028	0.074
	Trajectory Duration(s)	2.838	3.154	2.621
	Rotors Impulse(N·s)	41.260	45.879	30.699
(b)	Computation Time(s)	0.036	0.015	0.107
	Trajectory Duration(s)	2.838	3.599	2.654
	Rotors Impulse(N·s)	41.758	51.450	32.308

stems from our ground-effect compensation framework that strategically utilizes spring-leg dynamics through contact-aware optimization.

To validate the gait diversity, we conducted comparative x-z plane simulations during the stance phase against a passive SLIP model without rotor actuation. Under the same system parameters, including a mass of 1.5 kg, a spring stiffness coefficient of 400 N/m, and a leg length of 0.5 m, given the initial states with varying velocities and touch-down angles, gait optimization simulations verified symmetric trajectory formation - requiring matching initial/final horizontal velocity v_x with inverted vertical velocity v_y and take-off angle θ_{TO} . By enforcing symmetric kinematic constraints (e.g. velocity and touch down angle) before and after stance phases, this approach enables stable periodic gaits while satisfying foot placement requirements [23].

As demonstrated in Fig. 5(c), the passive SLIP model achieves stable symmetric trajectories only within limited initial states. In contrast, our rotors SLIP model expands the feasible initial state space for symmetric trajectories, bounded by the curved surface. Furthermore, parametric studies reveal a positive correlation between horizontal velocity magnitude and admissible touch-down angle range for stable hopping.

C. The Study of Hybrid Tracking Control

We validate the effectiveness of our control strategy through a comparative analysis with two baseline methods. The first baseline, w/o Actuators Impulse (following the approach of Wang [10] and Bai [11]), estimates state jumps during stance phases by only considering ground reaction forces while disabling rotor actuation during these phases. The second baseline, w/o Trajectory Extension, rigidly tracks the entire hybrid modal trajectory without applying our

TABLE III. A Comparison of Different Control Strategies

Scenario	Tracking Error ↓	w/o Actuators Impulse	w/o Trajectory Extension	Ours
(a)	RMSE(m)	0.039	0.052	0.027
	Max(m)	0.122	0.166	0.078
	RMSE-Z(m)	0.038	0.051	0.027
	Max-Z(m)	0.121	0.166	0.078
(b)	RMSE(m)	0.056	0.076	0.044
	Max(m)	0.143	0.171	0.095
	RMSE-Z(m)	0.044	0.063	0.036
	Max-Z(m)	0.117	0.171	0.094

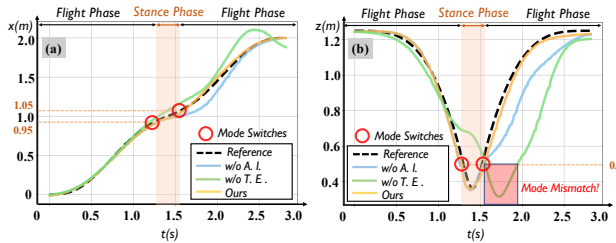


Fig. 7. Comparison of Tracking Performance in forward hopping scenario: (a) presents the comparison of x-axis position tracking performance; (b) presents the comparison of z-axis position tracking performance.

trajectory extension strategy. We repeated the simulation six times with each of the three control methods in two scenarios as shown in Fig. 6, tracking the dynamically feasible hybrid trajectories optimized by our methods.

Precise trajectory tracking minimizes landing position errors of legged quadrotors, critically enabling reliable terrestrial interaction during dynamic transitions, which is a fundamental requirement for executing sequential hybrid locomotion tasks in cluttered environments. The tracking error statistics from hybrid motion simulations across two scenarios are summarized in Table III and shown in Fig. 7. From these results, we draw two conclusions:

- i) Rotor actuation during stance phases significantly reduces trajectory tracking errors for spring-legged quadrotors.
- ii) The trajectory extension strategy ensures precise mode transitions through predictive contact management.

Although the rotor effects on positional errors during stance are minimal, the w/o Actuators Impulse method fails to provide adequate ascent velocity during subsequent flight phases. The absence of continuous rotor control during the previous stance phase leads to insufficient impulse accumulation, resulting in 27% larger positional errors compared to our approach. Regarding mode switching, the w/o Trajectory Extension method prematurely transitions to stance dynamics before actual ground contact, causing significant tracking divergence (0.076m RMSE vs. 0.044m in our method).

D. Real-world Experiment

Experimental validation confirms our framework's effectiveness for spring-legged quadrotors, demonstrating seamless aerial-terrestrial hybrid locomotion with three different stance gaits as shown in Fig. 1. The result of vertical hopping and forward hopping is shown in Fig. 8. In vertical hopping tests, the controller maintains consistent altitude tracking with the reference trajectory. During rapid descent transi-

tions to stance mode, optimized rotor thrust during spring compression reduces energy consumption while accurately tracking position/velocity commands. However, altitude recovery delays persist despite increased rotor thrust at stance termination, which we attribute to ground effects degrading performance without spring compensation.

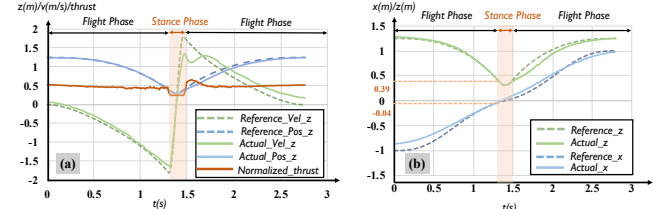


Fig. 8. Result on hybrid locomotion: (a) represents the z-axis vertical hopping experiment; (b) depicts the tracking performance in the x-z plane forward hopping experiment.

In forward hopping tests, the controller successfully executes hybrid locomotion with rapid mode transitions and accurate foothold placement near target locations, demonstrating the potential of spring-legged quadrotors for precise terrain sampling in constrained environments. Additionally, we demonstrate an emergency-stop hybrid motion trajectory that exploits ground contact torque to induce rapid directional reorientation of the spring-legged quadrotors.

VII. CONCLUSION

This study introduces a unified differential flatness framework for spring-legged quadrotors, integrating spring dynamics to enable smooth aerial-terrestrial locomotion. We develop a trajectory optimization method meeting agile, stance-gait diverse, and dynamically feasible requirements and an enhanced HNMPC architecture with a trajectory extension strategy, reducing tracking errors compared to existing methods. Extensive simulations and real-world experiments validate the approach's effectiveness in diverse hybrid locomotion. While the passive spring design improves aerial-terrestrial mobility, it limits stance phase duration. Future work will extend this framework to active-legged systems to enhance terrain adaptability through dynamic stiffness modulation.

REFERENCES

- [1] Y. Qin, Y. Li, X. Wei, and F. Zhang, "Hybrid aerial-ground locomotion with a single passive wheel," in 2020 IEEE/RSJ International Conference on Intelligent Robots and Systems (IROS). IEEE, 2020, pp. 1371–1376.
- [2] N. Pan, J. Jiang, R. Zhang, C. Xu, and F. Gao, "Skywalker: A compact and agile air-ground omnidirectional vehicle," *IEEE Robotics and Automation Letters*, vol. 8, no. 5, pp. 2534–2541, 2023.
- [3] K. Shi, Z. Jiang, L. Ma, L. Qi, and M. Jin, "Mtobot: An efficient morphable terrestrial-aerial robot with two transformable wheels," *IEEE Robotics and Automation Letters*, vol. 9, no. 2, pp. 1875–1882, 2024.
- [4] J. Lin, R. Zhang, N. Pan, C. Xu, and F. Gao, "Skater: A novel bi-modal bi-copter robot for adaptive locomotion in air and diverse terrain," *IEEE Robotics and Automation Letters*, 2024.
- [5] H. Xu, X. Zheng, Y. Wang, and L. Liao, "Flybot: A dual active wheel hybrid land-air robot with five-link leg joints," *IEEE Robotics and Automation Letters*, 2024.
- [6] K. Kim, P. Spieler, E.-S. Lupu, A. Ramezani, and S.-J. Chung, "A bipedal walking robot that can fly, slackline, and skateboard," *Science Robotics*, vol. 6, no. 59, p. eabf8136, 2021.

- [7] X. Zeng, G. Zhang, X. Ma, A. Xie, and Y. Li, "Design and control of the rotor-assisted planar folding-leg robot kou," *IEEE/ASME Transactions on Mechatronics*, 2024.
- [8] W. D. Shin, H.-V. Phan, M. A. Daley, A. J. Ijspeert, and D. Floreano, "Fast ground-to-air transition with avian-inspired multifunctional legs," *Nature*, vol. 636, no. 8041, pp. 86–91, 2024.
- [9] B. Zhu, J. Xu, A. Charway, and D. Saldaña, "Pogodrone: Design, model, and control of a jumping quadrotor," in *2022 International Conference on Robotics and Automation (ICRA)*. IEEE, 2022, pp. 2031–2037.
- [10] Y. Wang, J. Kang, Z. Chen, and X. Xiong, "Terrestrial locomotion of pogox: From hardware design to energy shaping and step-to-step dynamics based control," in *2024 IEEE International Conference on Robotics and Automation (ICRA)*. IEEE, 2024, pp. 3419–3425.
- [11] S. Bai, Q. Pan, R. Ding, H. Jia, Z. Yang, and P. Chirarattananon, "An agile monopedal hopping quadcopter with synergistic hybrid locomotion," *Science Robotics*, vol. 9, no. 89, p. eadi8912, 2024.
- [12] M. Nail, N. Jäne, O. Ma, G. Arellano, E. Atkins, and R. B. Gillespie, "Simplifying aerial manipulation using intentional collisions," in *2023 IEEE International Conference on Robotics and Automation (ICRA)*. IEEE, 2023, pp. 5359–5365.
- [13] K. Sugihara, M. Zhao, T. Nishio, T. Makabe, K. Okada, and M. Inaba, "Design and control of a small humanoid equipped with flight unit and wheels for multimodal locomotion," *IEEE Robotics and Automation Letters*, 2023.
- [14] Y. Zeng, Y. Huang, and X. Xiong, "Reference-steering via data-driven predictive control for hyper-accurate robotic flying-hopping locomotion," *arXiv preprint arXiv:2411.18793*, 2024.
- [15] H. Yu, H. Gao, and Z. Deng, "Toward a unified approximate analytical representation for spatially running spring-loaded inverted pendulum model," *IEEE Transactions on Robotics*, vol. 37, no. 2, pp. 691–698, 2020.
- [16] D. Mellinger and V. Kumar, "Minimum snap trajectory generation and control for quadrotors," in *2011 IEEE international conference on robotics and automation*. IEEE, 2011, pp. 2520–2525.
- [17] C. Richter, A. Bry, and N. Roy, "Polynomial trajectory planning for aggressive quadrotor flight in dense indoor environments," in *Robotics Research*. Springer, 2016, pp. 649–666.
- [18] S. Liu, M. Watterson, K. Mohta, K. Sun, S. Bhattacharya, C. J. Taylor, and V. Kumar, "Planning dynamically feasible trajectories for quadrotors using safe flight corridors in 3-d complex environments," *IEEE Robotics and Automation Letters*, vol. 2, no. 3, pp. 1688–1695, 2017.
- [19] M. Rijnen, A. Saccon, and H. Nijmeijer, "On optimal trajectory tracking for mechanical systems with unilateral constraints," in *2015 54th IEEE Conference on Decision and Control (CDC)*. IEEE, 2015, pp. 2561–2566.
- [20] F. Furrer, M. Burri, M. Achtelik, and R. Siegwart, *Robot Operating System (ROS): The Complete Reference (Volume 1)*. Cham: Springer International Publishing, 2016, ch. RotorS—A Modular Gazebo MAV Simulator Framework, pp. 595–625. [Online]. Available: http://dx.doi.org/10.1007/978-3-319-26054-9_23
- [21] S. G. Johnson, "The NLOpt nonlinear-optimization package," <https://github.com/stevengj/nlopt>, 2007.
- [22] F. Farshidian *et al.*, "OCS2: An open source library for optimal control of switched systems," [Online]. Available: <https://github.com/leggedrobotics/ocs2>.
- [23] G. Piovan and K. Byl, "Enforced symmetry of the stance phase for the spring-loaded inverted pendulum," in *2012 IEEE International Conference on Robotics and Automation*. IEEE, 2012, pp. 1908–1914.